

See discussions, stats, and author profiles for this publication at: <https://www.researchgate.net/publication/261699873>

A Schiff Base and Its Cu(II) Complex as Highly Selective Chemodosimeter for Hg(II) Involving Preferential Hydrolysis of Aldimine Over Ester Group

ARTICLE *in* INORGANIC CHEMISTRY · APRIL 2014

Impact Factor: 4.76

READS

51

7 AUTHORS, INCLUDING:



Mrigendra Dubey

Indian Institute of Technology (Banaras Hindu...)

19 PUBLICATIONS 37 CITATIONS

[SEE PROFILE](#)



Rakesh Kumar Gupta

Kyushu University

29 PUBLICATIONS 201 CITATIONS

[SEE PROFILE](#)



Alok Ch. Kalita

Kaziranga University

14 PUBLICATIONS 40 CITATIONS

[SEE PROFILE](#)



Daya Shankar Pandey

Banaras Hindu University

93 PUBLICATIONS 1,116 CITATIONS

[SEE PROFILE](#)

A Schiff Base and Its Copper(II) Complex as a Highly Selective Chemodosimeter for Mercury(II) Involving Preferential Hydrolysis of Aldimine over an Ester Group

Ashish Kumar,[†] Mrigendra Dubey,[†] Rampal Pandey,[‡] Rakesh Kumar Gupta,[†] Amit Kumar,[†] Alok Ch. Kalita,[§] and Daya Shankar Pandey*,[†]

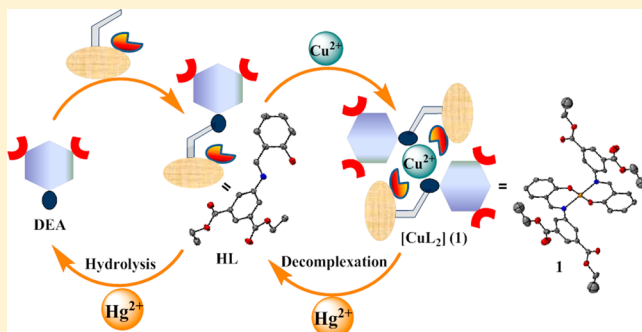
[†]Department of Chemistry, Faculty of Science, Banaras Hindu University, Varanasi 221 005, U.P., India

[‡]Department of Chemistry, Dr. Hari Singh Gour University, Sagar 470 003, M.P., India

[§]Department of Chemistry, Indian Institute of Technology, Bombay 400 076, Maharashtra, India

Supporting Information

ABSTRACT: The syntheses of a new Schiff base, diethyl-5-(2-hydroxybenzylidene)aminoisophthalate (**HL**), and a copper complex, $[\text{Cu}(\text{L}_2)]$ (**1**), imparting L^- , have been described. Both the ligand **HL** and complex **1** have been thoroughly characterized by elemental analyses, electrospray ionization mass spectrometry, FT-IR, NMR (^1H and ^{13}C), electronic absorption, and emission spectral studies and their structures determined by X-ray single-crystal analyses. Distinctive chemodosimetric behavior of **HL** and **1** toward Hg^{2+} has been established by UV-vis, emission, and mass spectral studies. Comparative studies further revealed that the chemodosimetric response solely originates from selective hydrolysis of the aldimine moiety over the ester group and **1** exhibited greater selectivity toward Hg^{2+} relative to **HL** while the sensitivity order is reversed. Further, these followed different hydrolytic pathways but ended up with the same product analyzed for diethyl-5-aminoisophthalate (DEA). Hg^{2+} -induced displacement of Cu^{2+} and subsequent hydrolysis of the $-\text{HC}=\text{N}-$ moiety in **1** affirmed the identity of the actual species undergoing hydrolysis as **HL**. The occurrence of Cu^{2+} displacement and Hg^{2+} detection via hydrolytic transformation has been supported by various physicochemical studies.



INTRODUCTION

Studies pertaining to the detection and determination of heavy- and transition-metal ions have been attractive because of their extremely toxic impact on the environment and biological systems.¹ Among these, mercury presents one of the most hazardous and toxic pollutants that upon inhaling or ingestion poses serious health problems.^{2,3} Regardless of the toxicity, mercury and its salts find wide applications in diverse industrial processes and products like paints, electronic equipment, and batteries.^{4,5} Although strict regulations have decreased its use in many industrial processes, a high concentration of mercury is still present in many environmental segments.⁶ Amid different forms of mercury distributed in the environment (Hg^0 , Hg^{2+} , and CH_3Hg^+), methyl mercury easily enters the food chain of aquatic organisms and ultimately in human beings.⁷ Bioaccumulation of methyl mercury occurs to a greater extent relative to its elemental and inorganic forms, and its buildup in the liver, kidney, and spleen even at lower concentrations leads to DNA damage, mitosis impairment, and nervous system defects.⁸ Therefore, the development of suitable techniques for its detection and determination has been a challenging task.⁹ Further, owing to its d^{10} configuration, Hg^{2+} lacks an optical spectroscopic signature and its optical detection is achieved by

monitoring Hg^{2+} -induced changes in the UV-vis or fluorescence of a chromophore.¹⁰

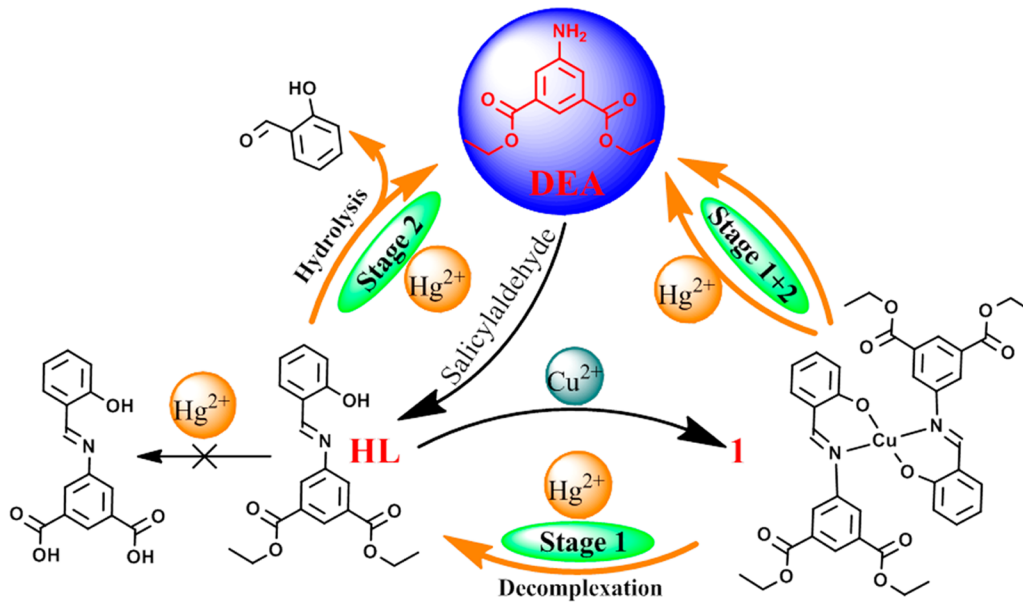
Considering these issues, various novel molecules (fluorophores,^{11–17} proteins,¹⁸ and metal nanoparticles¹⁹) have been synthesized and used toward the development of techniques for the detection of Hg^{2+} . These methods also bear a scope of overcoming some unavoidable limitations such as poor solubility, cross-sensitivity of other metal ions, and cost effectiveness of the probe synthesis. Continual efforts in this direction have led to the manifestation of a chemodosimetric approach for the detection of Hg^{2+} .²⁰ Efficacy of this approach largely depends upon the elegant design of probes capable of exhibiting highly selective and sensitive spectroscopic responses to Hg^{2+} -induced chemical transformations. In this context, a few systems have been devised that can selectively detect Hg^{2+} in an aqueous/mixed-aqueous media via hydrolytic transformation of the Schiff base.²¹ Moreover, to best of our knowledge, none of the available systems involve Hg^{2+} -assisted preferential cleavage of the aldimine bond over ester groups. In search of such a “turn-on” fluorescent chemodosimeter for

Received: December 26, 2013

Published: April 28, 2014



Chart 1



Hg^{2+} in mixed-aqueous media, a new Schiff base, diethyl-5-(2-hydroxybenzylidene)aminoisophthalate (**HL**), and a copper(II) complex, $[\text{Cu}(\text{L}_2)]$ (**1**), containing L^- have been synthesized.

Through this contribution, we present aldimine-based systems **HL** and **1**, which accomplish the detection of Hg^{2+} through hydrolysis at a specific aldimine site without affecting the ester groups under a suitable pH range ($\sim 7.2\text{--}3.5$) in mixed-aqueous media. The mechanistic pathways (Chart 1) have been profoundly established by various methods, which strongly support Hg^{2+} -induced Cu^{2+} displacement *cum* explicit hydrolysis at the $-\text{HC}=\text{N}-$ bond and accountability of the resulting species (diethyl-5-aminoisophthalate, **DEA**) for a fluorescence "turn-on" response toward Hg^{2+} .

EXPERIMENTAL SECTION

Materials. Solvents were dried and distilled prior to their use following standard procedures.²² Reagent-grade chemicals were used throughout, and HPLC-grade solvents were employed for spectroscopic studies. The metal nitrates $\text{Hg}(\text{NO}_3)_2 \cdot 2\text{H}_2\text{O}$ (98.0% purity) and $\text{Cu}(\text{NO}_3)_2 \cdot 2.5\text{H}_2\text{O}$ were purchased from Sigma-Aldrich Chemical Co. Pvt. Ltd. and used as received. Diethyl-5-aminoisophthalate (**DEA**) was prepared following a literature procedure with slight modifications.²³

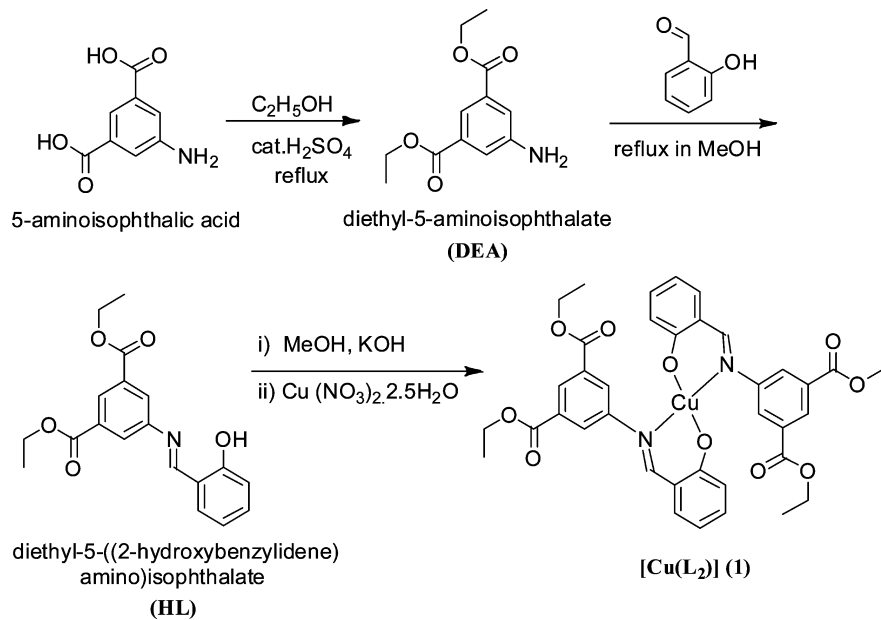
Physical Measurements. Elemental analyses on the samples were performed in the Microanalytical Laboratory of the Department of Chemistry, Faculty of Science, Banaras Hindu University, Varanasi, India, on an Exeter Analytical Inc. CE-440 analyzer. IR and electronic absorption spectra were acquired on PerkinElmer 577 FT-IR and Shimadzu UV-1601 spectrophotometers, respectively. ¹H (300 MHz) and ¹³C (75.45 MHz) NMR spectra were obtained at room temperature (rt) on a JEOL AL300 FT-NMR spectrometer using tetramethylsilane [TMS, $\text{Si}(\text{CH}_3)_4$] as an internal reference. Emission spectra at rt were recorded on a PerkinElmer fluorescence spectrometer (LS-55) in methanol ($\text{MeOH}/\text{H}_2\text{O}$ (9:1, v/v). Electrospray ionization mass spectrometric (ESI-MS) data were acquired on Bruker Micro TOF QII and THERMO Finnigan LCQ Advantage Max ion-trap mass spectrometers.

Preparation of DEA. A solution of 5-aminoisophthalic acid (5.0 g, 27.62 mmol) in dry ethanol (50 mL) was treated with concentrated sulfuric acid (4 mL) and the resulting solution heated under reflux for 16 h. The reaction mixture was poured into ice–water containing sodium hydrogen carbonate (10.0 g), and the white precipitate thus

obtained was filtered, washed several times with water, extracted with dichloromethane, and dried using anhydrous Na_2SO_4 . After decantation, the filtrate was concentrated to dryness under reduced pressure on a rotary evaporator to afford the desired product. Yield: 4.7 g, 72%. Anal. Calcd for $[\text{C}_{12}\text{H}_{15}\text{NO}_4]$: C, 60.75; H, 6.37; N, 5.90. Found: C, 60.63; H, 6.31; N, 5.86. IR (KBr pellets, cm^{-1}): 3457 and 3363 (s, $\text{N}-\text{H}_{\text{str}}$, ArNH_2), 2997–2905 (m, $\nu_{\text{str}} \text{C}-\text{H}_{\text{aliphatic}}$), 1698 and 1689 (s, $\nu_{\text{str}} \text{C}=\text{O}_{\text{ester}}$). ¹H NMR (CDCl_3 , 300 MHz, δ_{H} ppm): 8.05 (s, 1H, ArH), 7.51 (s, 2H, ArH), 4.37 (m, 2H, $J = 6.9$ Hz, CH_2), 3.97 (br, 2H, NH_2), 1.39 (t, 3H, $J = 6.9$ Hz, CH_3). ¹³C NMR (CDCl_3 , 75.45 MHz, δ_{C} ppm): 166.1, 146.6, 131.7, 120.5, 120.4, 119.6, 61.2, 14.3. UV-vis [c , 50 μM ; 9:1 (v/v) $\text{MeOH}/\text{H}_2\text{O}$; λ_{max} nm (ϵ , $\text{M}^{-1} \text{cm}^{-1}$)]: 330 (7.70 \times 10³), 252 (1.67 \times 10⁴).

Synthesis of Diethyl-5-(2-hydroxybenzylidene)-aminoisophthalate (HL**).** **DEA** (1.185 g, 5.0 mmol) dissolved in MeOH (50 mL) was added dropwise to a methanolic solution (10 mL) of salicylaldehyde (0.53 mL, 5.0 mmol) and the resulting solution heated under reflux for 12 h. The reaction mixture was filtered while hot and its volume reduced to ~ 20 mL. A few drops of acetonitrile was added to the above solution and allowed to cool at rt. This afforded diffraction-quality yellow block-shaped crystals within 5 h. Yield: 1.2 g, 69%. Anal. Calcd for $[\text{C}_{19}\text{H}_{19}\text{NO}_5]$: C, 66.85; H, 5.61; N, 4.10. Found: C, 66.79; H, 5.59; N, 4.02. IR (KBr pellets, cm^{-1}): 2993–2876 (m, $\nu_{\text{str}} \text{C}-\text{H}_{\text{aliphatic}}$), 1722–1710 (vs, $\nu_{\text{str}} \text{C}=\text{O}_{\text{ester}}$), 1619 (s, $\nu_{\text{str}} \text{C}=\text{N}$). ¹H NMR (CDCl_3 , 300 MHz, δ_{H} ppm): 12.82 (s, 1H, H_9), 8.71 (s, 1H, H_4), 8.58 (s, 1H, H_1), 8.12 (s, 2H, H_2 and H_3), 7.42 (t, 2H, H_5 and H_8), 6.99 (m, 2H, H_6 and H_7), 4.44 (q, 4H, $J = 6.9$ Hz, H_{10}), 1.44 (t, 6H, $J = 6.9$ Hz, H_{11}). ¹³C NMR (CDCl_3 , 75.45 MHz, δ_{C} ppm): 165.3, 164.4, 161.1, 148.9, 133.8, 132.7, 132.2, 128.5, 126.2, 119.2, 118.8, 117.3, 61.6, 14.2. ESI-MS (rel intens). Calcd, found: m/z 342.1341, 342.1518 [($\text{M} + \text{H}$)⁺, 100%]. UV-vis [c , 50 μM ; 9:1 (v/v) $\text{MeOH}/\text{H}_2\text{O}$; pH ~ 7.2 ; λ_{max} nm (ϵ , $\text{M}^{-1} \text{cm}^{-1}$)]: 338 (1.24 \times 10⁴), 274 (1.77 \times 10⁴).

Synthesis of $[\text{Cu}(\text{L}_2)]$ (1**).** To a deprotonated solution of **HL** [obtained by treating **HL** (1.023 g, 3.0 mmol) with KOH (0.168 g, 3.0 mmol) in MeOH (50 mL) and stirring for 20 min to afford a clear yellow solution] was added with stirring a methanolic solution of $\text{Cu}(\text{NO}_3)_2 \cdot 2.5\text{H}_2\text{O}$ (0.350 g, 1.5 mmol, 5 mL). Immediately, the color of the reaction mixture turned olive green, and a precipitate started to appear within 10 min. This was stirred for an additional 3 h and the resulting precipitate filtered and washed with cooled MeOH and diethyl ether. The crude solid thus obtained upon crystallization from tetrahydrofuran (THF)/methyl cyanide (MeCN) (9:1, v/v) afforded block-shaped green crystals within 2 days. These were separated and

Scheme 1. Synthesis of **HL** and **1**

dried in vacuo. Yield: 0.621 g, 55%. Anal. Calcd for $[\text{C}_{38}\text{H}_{36}\text{CuN}_2\text{O}_{10}]$: C, 61.32; H, 4.88; N, 3.76. Found C, 61.24; H, 4.96; N, 3.69. IR (KBr pellets, cm^{-1}): 2954 (m, ν_{str} C—H_{aliphatic}), 1723 (vs, ν_{str} C=O_{ester}), 1613 (s, ν_{str} C=N). ESI-MS (rel intens). Calcd, found: m/z 745.2538, 745.2052 [(M + H)⁺]. UV/vis [c , 50 μM ; 9:1 (v/v) MeOH/H₂O; pH ~7.4; λ_{max} nm (ϵ , $\text{M}^{-1} \text{cm}^{-1}$)]: 392 (1.09 $\times 10^4$), 281 (3.16 $\times 10^4$).

UV/vis and Fluorescence Studies. A stock solution of **HL** and **1** for electronic absorption (50 μM) and fluorescence (10 μM) studies was prepared in 9:1 (v/v) MeOH/H₂O. Solutions of the respective metal ions (Na^+ , K^+ , Mg^{2+} , Ca^{2+} , Mn^{2+} , Co^{2+} , Ni^{2+} , Cu^{2+} , Ag^+ , Zn^{2+} , Cd^{2+} , Hg^{2+} , and Pb^{2+}) were prepared by dissolving their nitrate salts in triply distilled water (100 mM). In a typical titration, a solution of **HL** and **1** was taken in a quartz cuvette (3.0 mL; path length, 1 cm), and diluted stock solutions of the metal ions were added gradually with the help of a micropipet. The spectral changes for **HL** and **1** were noted as a function of the equivalents of the metal ions added after 2 min, and all of the experiments were repeated thrice.

Crystal Structure Determinations. Suitable crystals for single-crystal X-ray diffraction analyses for **HL** were obtained directly from the reaction mixture and for **1** using THF/MeCN (9:1, v/v). The crystals were mounted on glass fibers. All of the geometric and intensity data were collected at 150 K using a Rigaku Saturn 724+ CCD diffractometer with a fine-focus 1.75 kW sealed tube Mo $\text{K}\alpha$ ($\lambda = 0.71075 \text{ \AA}$) X-ray source, with increasing ω (width of 0.3 per frame) at a scan speed of either 3 or 5 s/frame. After the initial solution, refinement was performed with a *WinGX* environment using direct methods (*SHELXS* 97) and by full-matrix least squares on F^2 (*SHELX* 97).²⁴ All of the non-hydrogen atoms were refined anisotropically, and hydrogen atoms were geometrically fixed and refined as per the riding model.

RESULTS AND DISCUSSION

Synthesis and Characterization. The ligand **HL** was synthesized by condensation of **DEA** with salicylaldehyde (1:1) in MeOH under refluxing conditions in ~69% yield [Supporting Information (SI), Figures S1 and S2]. After cooling to rt, the reaction mixture, upon treatment with a few drops of acetonitrile and allowing it to remain undisturbed, gave yellow block-shaped crystals within 5 h. The deprotonated ligand L^- [obtained by treating **HL** with potassium hydroxide (KOH) in MeOH and stirring for 20 min; see the Experimental Section] reacted with hydrated $\text{Cu}(\text{NO}_3)_2 \cdot 2.5\text{H}_2\text{O}$ (2:1) to

afford the mononuclear complex **1** in good yield (55%). A simple scheme showing the synthesis of **HL** and **1** is depicted in Scheme 1.

Characterization of **HL** and **1** has been achieved by satisfactory elemental analyses and spectral (IR, NMR, UV/vis, fluorescence, and ESI-MS) studies. Crystal structures of both **HL** and **1** have been authenticated by X-ray single-crystal analyses.

The ¹H NMR spectrum of **HL** is expected to exhibit singlets due to the phenolic (—OH) and aldimine (—HC=N—) protons in downfield side along with other protons. Expectedly, it displayed two distinct singlets at δ 12.82 (—OH) and 8.71 (—CH=N—). The isophthalate ring protons resonated as singlets at δ 8.58 (H1) and 8.12 (H2 and H3), while phenolic ring protons (H5, H6, H7, and H8) resonated as a multiplet at $\sim\delta$ 7.45–6.95. In addition, methylene and methyl protons appeared as a quartet and a triplet at δ 4.44 (4H) and 1.44 (6H), respectively. The position and integrated intensity of various signals in the ¹H NMR spectrum strongly supported the formulation of ligand **HL**. ¹³C NMR spectral data (summarized in the Experimental Section) also corroborated well with the formation of **HL** (SI, Figure S2). The composition of both **HL** and **1** has also been supported by ESI-MS studies (SI, Figure S4). Molecular ion peaks at m/z 342.1518 [(M + H)⁺, 100%] and 745.2052 [(M + H)⁺, 25%], respectively, in the ESI-MS spectra of **HL** and **1** strongly supported their formulations (vide supra).

Crystal Structures of **HL and **1**.** The ligand **HL** crystallizes in an orthorhombic system and space group $Pca2_1$ and **1** in a monoclinic system with space group $P2_1/c$. Selected crystallographic data and geometrical parameters for these are summarized in Tables 1 and S1 (SI), respectively, and their pertinent views along with the atom numbering scheme (partial) are depicted in Figures 1 and 2. The crystal structure of **HL** revealed that it is a nonplanar molecule, wherein isophthalate and phenolic rings are mutually twisted with a dihedral angle of 43.32° (SI, Figure S5). This twisting may enhance the photoinduced electron-transfer (PET) phenomenon responsible for fluorescence quenching.²⁵

Table 1. Crystal Data and Structure Refinements for Ligand HL and Complex 1

	HL	1
identification code	SHELXL	SHELXL
empirical formula	C ₁₉ H ₁₉ NO ₅	C ₃₈ H ₃₆ CuN ₂ O ₁₀
fw	341.35	744.23
temperature (K)	150(2)	150(2)
wavelength (Å)	0.71075	0.71075
cryst syst	orthorhombic	monoclinic
space group	Pca ₂ ₁	P2 ₁ /c
unit cell dimens		
a (Å)	7.616(2)	14.870(10)
b (Å)	13.133(5)	7.459(6)
c (Å)	16.922(6)	14.326(9)
α (deg)	90	90
β (deg)	90	90.468(11)
γ (deg)	90	90
volume (Å ³)	1692.6(10)	1588.9(19)
Z	4	2
density (calcd)(mg m ⁻³)	1.340	1.556
abs coeff (mm ⁻¹)	0.097	0.756
F(000)	720	774
cryst size (mm ³)	0.10 × 0.10 × 0.04	0.08 × 0.04 × 0.02
θ range for data collection (deg)	2.86–24.99	2.74–25.00
reflns collected	11887	11476
indep reflns	2957 [R(int) = 0.0319]	2787 [R(int) = 0.0572]
completeness to $\theta = 24.99^\circ$ (%)	99.90	99.70
abs corrn	semiempirical from equivalents	semiempirical from equivalents
max and min transmission	0.9961 and 0.9903	0.9850 and 0.9420
refinement method	full-matrix least squares on F^2	full-matrix least squares on F^2
data/restraints/param	2957/1/226	2787/23/232
GOF on F^2	0.976	1.132
final R indices [$I > 2\sigma(I)$]	R1 = 0.0353, wR2 = 0.0789	R1 = 0.0881, wR2 = 0.2255
R indices (all data)	R1 = 0.0380, wR2 = 0.0805	R1 = 0.1005, wR2 = 0.2355
largest diff peak and hole (e Å ⁻³)	0.126 and -0.153	0.929 and -1.323

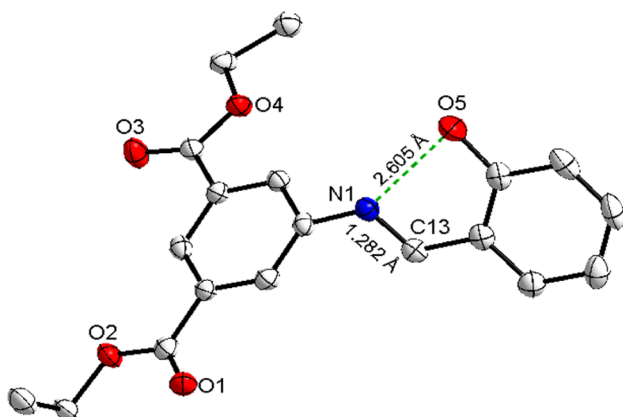


Figure 1. ORTEP view of HL showing intramolecular hydrogen bonding (50% ellipsoid probability and hydrogen atoms omitted for clarity).

The phenolic $-\text{OH}$ (donor) and azomethine nitrogen (acceptor) atoms are involved in intramolecular hydrogen

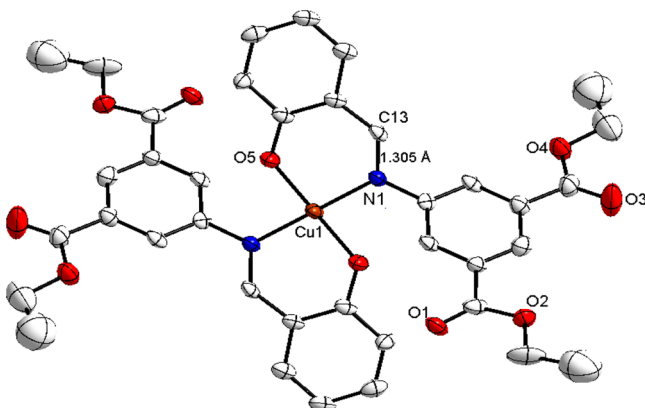


Figure 2. ORTEP view of 1 (50% probability and hydrogen atoms omitted for clarity).

bonding with an interaction distance of 2.605 Å. This lies within the range for O–H···N hydrogen bond distances.²⁶ In the crystal lattice, molecular units adopt a zigzag arrangement originating from an alternate array of successive isophthalate ring planes (SI, Figure S6). Various bond distances and angles fall within the typical range reported for analogous systems.²⁷

The copper(II) center in 1 assumes a square-planar geometry completed by phenolate oxygen and aldimine nitrogen from deprotonated ligand L[−] in a trans N₂O₂ fashion (Figure 2). The dihedral angle between the isophthalate and phenolate ring planes in a particular ligand unit is 46.48°, which is comparable to that in HL (SI, Figure S5). The Cu–O (1.889 Å) and Cu–N (2.021 Å) bond distances and angles lie within the acceptable range and are comparable to those in other related systems.²⁸ The aldimine bond lengths C13–N1 in both HL (1.282 Å) and 1 (1.305 Å) also corroborated well with analogous systems.²⁷ Further, HL lacks any solvent molecules and intermolecular weak interactions like hydrogen bonding and π ··· π stacking, while 1 shows strong stacking between the phenolate–isophthalate and phenolate–phenolate rings with stacking distances of 3.631 and 3.577 Å, respectively.

Absorption and Emission Studies. The electronic absorption spectrum of HL [c , 50 μM; 9:1 (v/v) MeOH/H₂O; pH ~7.2] exhibited two prominent bands at 338 nm (ϵ , $1.24 \times 10^4 \text{ M}^{-1} \text{ cm}^{-1}$) and 274 nm (ϵ , $1.77 \times 10^4 \text{ M}^{-1} \text{ cm}^{-1}$). The low-energy (LE) band at 338 nm has been tentatively assigned to n–π* transitions and the high-energy (HE) band at 274 nm to the π–π* transitions.²⁹ To examine the interaction of HL with various cations, a solution of this compound was treated with 10.0 equiv of nitrate salts of Na⁺, K⁺, Mg²⁺, Ca²⁺, Mn²⁺, Co²⁺, Ni²⁺, Zn²⁺, Cd²⁺, Ag⁺, Pb²⁺, Cu²⁺, and Hg²⁺. This exhibited insignificant changes in the presence of the aforesaid metal ions except for Cu²⁺ and Hg²⁺ (Figure 3a). The addition of Hg²⁺ induced significant hypso- and hypochromic shifts ($\Delta\lambda$, 08 nm; $\Delta\epsilon$, $4.22 \times 10^3 \text{ M}^{-1} \text{ cm}^{-1}$) for the LE band. On the other hand, the HE band (λ , 274 nm) disappeared, and simultaneously a new band appeared at 252 nm (ϵ , $1.79 \times 10^4 \text{ M}^{-1} \text{ cm}^{-1}$). Likewise, the addition of the Cu²⁺ led to a decrease in the intensity of the LE band ($\Delta\epsilon$, $6.02 \times 10^3 \text{ M}^{-1} \text{ cm}^{-1}$); at the same time, the optical density of the HE band ($\Delta\epsilon$, $6.00 \times 10^2 \text{ M}^{-1} \text{ cm}^{-1}$) was enhanced with concomitant emergence of a new band at 392 nm (ϵ , $4.98 \times 10^3 \text{ M}^{-1} \text{ cm}^{-1}$). A significant shift in the position of the LE band and vanishing of the HE band in the presence of Hg²⁺ suggested noteworthy changes in the structure of HL. Conversely, in the presence of Cu²⁺, the

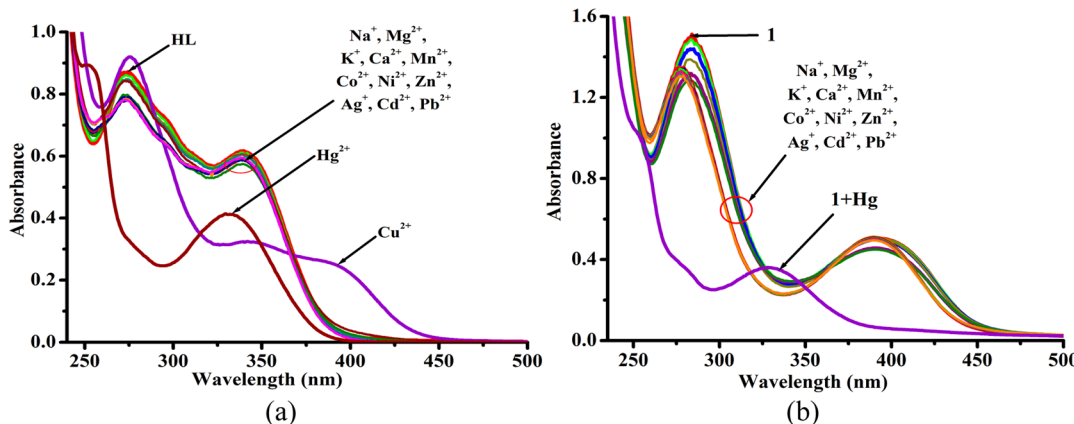


Figure 3. (a) Absorption spectra of **HL** (*c*, 50 μM) and in the presence of various metal ions. (b) Absorption spectra of **1** (*c*, 50 μM) with various metal ions (10.0 equiv) in MeOH/H₂O (9:1, v/v).

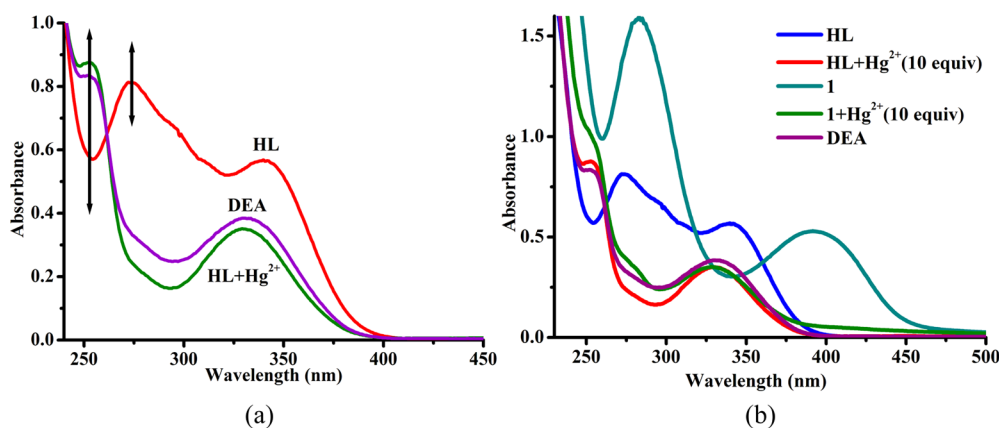


Figure 4. (a) Comparison of the absorption spectrum of **HL** + Hg²⁺ (green) with that of DEA (violet). (b) Resemblance of **HL** and **1** with each other after the addition of Hg²⁺ and their resemblance with DEA (violet).

intensity of the LE band appreciably decreased probably because of its interaction with **HL** through azomethine nitrogen and phenolic oxygen to form complex **1**.

On the basis of the disparity of spectral features, it may be concluded that **HL** interacted with Hg²⁺ and Cu²⁺ in a distinct manner. Changes in the UV/vis spectrum of **HL** selectively in the presence of Hg²⁺ and Cu²⁺ motivated us to investigate the ultimate product under harsh competition between Hg²⁺ and Cu²⁺. In this context, Hg²⁺ (10.0 equiv) and Cu²⁺ (10.0 equiv) were added to a solution of **HL** + Cu²⁺ (10.0 equiv) and **HL** + Hg²⁺ (10.0 equiv), respectively. In the first instance, spectral features were found to be similar to that of **HL** + Hg²⁺, while the second one remained unperturbed. This observation strongly suggested that the addition of Hg²⁺ causes similar effects on **HL** and **HL** + Cu²⁺. At this stage, we assume that Cu²⁺ is being displaced from the **HL** + Cu²⁺ complex by Hg²⁺ liberating the ligand under a reaction medium, which, in turn, undergoes hydrolytic cleavage.¹³ Moreover, **HL** possesses two dissimilar hydrolyzable sites in the form of an aldimine and two ester groups. Therefore, to validate the site of hydrolysis, the UV/vis spectrum of DEA itself was acquired. Notably, it came out to be similar to that of **HL** + Hg²⁺ or **HL** + Cu²⁺ + Hg²⁺, indicating hydrolytic cleavage of the aldimine bond (Figure 4a). Irrefutably, the addition of Hg²⁺ directly to a solution of **HL** induces hydrolysis at the aldimine bond, generating DEA, whereas it displaces Cu²⁺ from the **HL** + Cu²⁺ complex,

followed by hydrolysis at the aldimine linkage of the resulting **HL**.

With an objective of establishing the role of Cu²⁺ and Hg²⁺, we intended to synthesize the Cu²⁺ complex, imparting **HL**. The key idea behind this objective was to look into comparative affinities of the “aldimine” and “ester” functionalities toward the hydrolytic detection of Hg²⁺, particularly, in a protected aldimine site coordinated to Cu²⁺. In this regard, the desired copper complex **1** was synthesized and thoroughly characterized (vide supra). The electronic absorption spectrum of **1** comprises two intense bands at 392 and 281 nm due to n-π* and π-π* transitions, respectively (Figure 3b).

The addition of tested metal ions (10.0 equiv) to a solution of **1** displayed insignificant alterations in the spectral features of this complex except for Hg²⁺, which led to the loss of both LE and HE bands and the emergence of new bands at 330 and 252 nm, resembling that of DEA (Figure 3b). This observation strongly suggested that DEA is the ultimate product that arises from the interaction of both **HL** and **1** with Hg²⁺ (Figure 4b). This further strengthened the possibility of Hg²⁺-induced decomplexation of **1** followed by liberation of **HL** in the reaction medium, which, in turn, undergoes site-selective hydrolysis at the aldimine bond. Also, it strongly supported the Hg²⁺-selective *chemodosimetric behavior* of **HL** and **1** involving site-specific hydrolysis.^{20,21,30}

The ligand **HL** [*c*, 10 μM; 9:1 (v/v) MeOH/H₂O; pH ~7.2] and **1** [*c*, 10 μM; 9:1 (v/v) MeOH/H₂O; pH ~7.4] upon

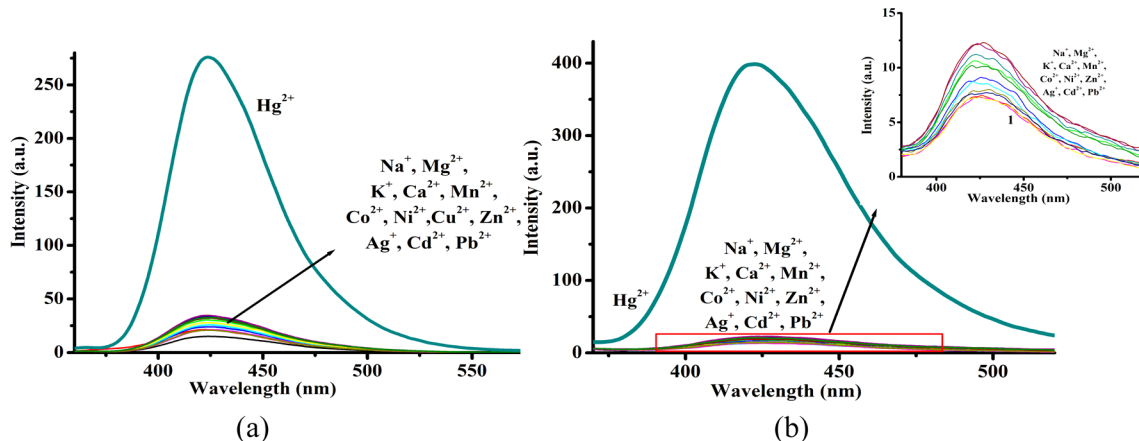


Figure 5. Fluorescence spectra of (a) **HL** (c , 10 μM) and (b) **1** (c , 10 μM) in the presence of various metal ions (10.0 equiv; c , 10 mM) in MeOH/H₂O (9:1, v/v).

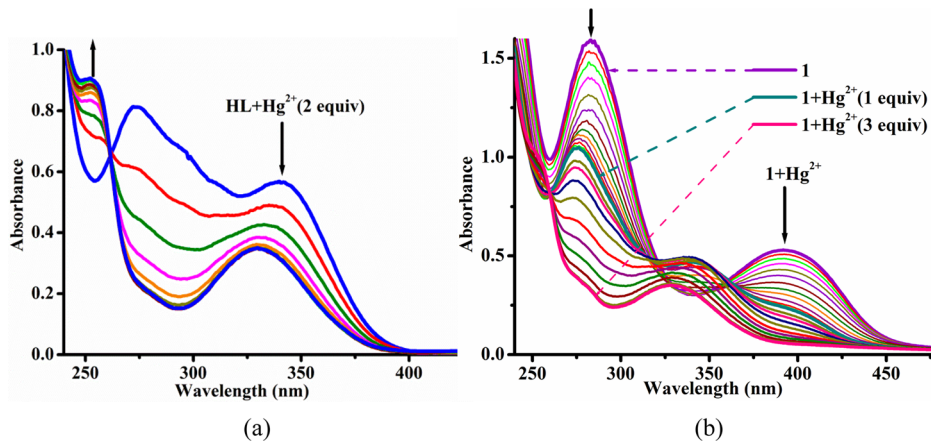


Figure 6. Absorption titration of (a) **HL** (c , 50 μM) and (b) **1** (c , 50 μM) in [9:1 (v/v) MeOH/H₂O] in the presence of Hg^{2+} (10 mM) at rt.

excitation at 338 nm weakly fluoresce ($\lambda_{\text{em}} = 423$ nm; Φ , 0.014, **HL**; $\lambda_{\text{em}} = 423$ nm; Φ , 0.011, **1**) with a Stokes shift of 85 nm. To compare and contrast the results, solutions of both **HL** and **1** were treated with tested metal ions under analogous conditions and excited at the same wavelength ($\lambda_{\text{ex}} = 338$ nm).^{13,31} Additionally, **1** was not excited at the LE band (392 nm) because it overlaps with its own emission bands ($\lambda_{\text{em}} = 423$ nm).

Both **HL** and **1** illustrated insignificant changes in their fluorescence spectra in the presence of tested metal ions (10.0 equiv) except for Hg^{2+} . Further, **HL** + Hg^{2+} leads to a \sim 30-fold enhancement (Φ , 0.43) in the fluorescence quantum yield (QY); however, a very small quenching was observed with Cu^{2+} . Likewise, the addition of Hg^{2+} to a solution of **1** causes \sim 55-fold (Φ , 0.62) emission enhancement (Figure 5a,b). Although both **HL** and **1** displayed good selectivity toward Hg^{2+} , comparative spectral (UV-vis and fluorescence) responses revealed that the latter exhibits greater selectivity and the former higher sensitivity toward Hg^{2+} . This may be ascribed to the unavailability of the aldimine moiety for interaction with other metal ions because of its involvement in complexation with the Cu^{2+} center.

Chemodosimetric Detection of Hg^{2+} . To scrutinize the quantitative chemodosimetric feasibility and sensitivity of **HL** and **1** toward Hg^{2+} , electronic absorption and fluorescence titration studies have been carried out. The addition of Hg^{2+} (0.2 equiv) to a solution of **HL** [c , 50 μM ; 9:1 (v/v) MeOH/

H₂O; pH \sim 7.2] exhibited a hypochromic shift ($\Delta\epsilon$, 1.54×10^3 M $^{-1}$ cm $^{-1}$) for the band at 338 nm with a negligible blue shift and substantial shrinkage of the band at 274 nm ($\Delta\epsilon$, 4.04×10^3 M $^{-1}$ cm $^{-1}$). Further additions of Hg^{2+} (0.3–2.0 equiv) led to complete loss of the band at 274 nm. At the same time, the optical density of the band at 338 nm significantly diminished with a concomitant hypsochromic shift (330 nm; $\Delta\lambda$, 08 nm; $\Delta\epsilon$, 4.22×10^3 M $^{-1}$ cm $^{-1}$) and a new band emerged at 252 nm (ϵ , 1.79×10^4 M $^{-1}$ cm $^{-1}$) (Figure 6a).

The isosbestic point at 262 nm signifies the existence of more than two species in the system. Saturation was attained at 2.0 equiv of Hg^{2+} quantification that may be accredited to generation of the hydrolyzed amine counterpart (DEA) to its maximum, through specific hydrolysis of the aldimine linkage of **HL**. The resulting species after isolation and thorough characterization by ¹H NMR and mass spectral studies was confirmed as DEA (SI, Figures S15a and S16). To ascertain applicability of **HL** as a selective chemodosimeter for Hg^{2+} , interference studies were carried out that demonstrated insignificant changes in the spectral features due to **HL** + Hg^{2+} and showed almost the same optical density at 338 nm (Figure 7a,b).

Similarly, the gradual addition of Hg^{2+} (1.0 equiv) to a solution of **1** [c , 50 μM ; 9:1 (v/v) MeOH/H₂O; pH 7.42] led to a hypochromic shift for the bands at 392 nm ($\Delta\epsilon$, 5.78×10^3 M $^{-1}$ cm $^{-1}$) and 281 nm ($\Delta\epsilon$, 1.15×10^4 M $^{-1}$ cm $^{-1}$). This was accompanied by the surfacing of a new band at 338 nm (ϵ , 9.32

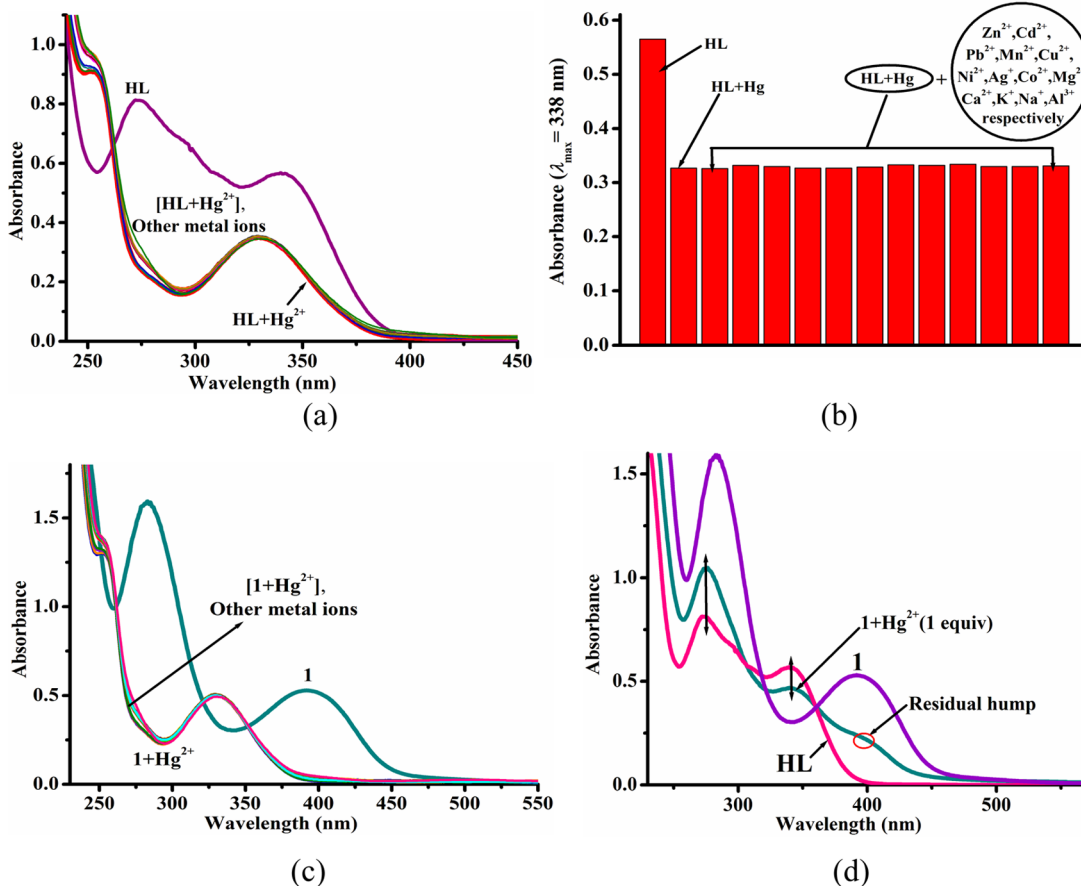


Figure 7. (a) Interference of various metal ions with Hg^{2+} in **HL**. (b) Bar diagram showing negligible interference of the other analytes with **HL** + Hg^{2+} at $\lambda = 338 \text{ nm}$. (c) Interference of various metal ions with Hg^{2+} in **1**. (d) Absorption spectrum of **1** after the addition of a Hg^{2+} solution (1.0 equiv) and its resemblance with **HL**.

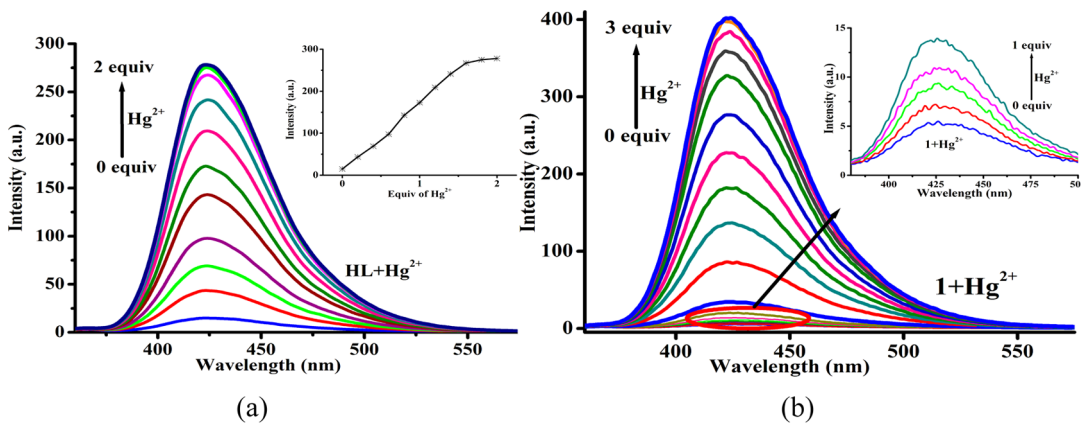


Figure 8. (a) Fluorescence titration of **HL** [9:1 (v/v) MeOH/H₂O; $c, 10 \mu\text{M}$]. The inset shows the intensity saturation curve for **HL** with equivalents of Hg^{2+} . (b) Fluorescence titration of **1** [9:1 (v/v) MeOH/H₂O, $c, 10 \mu\text{M}$] in the presence of Hg^{2+} (10 mM) at rt. The inset shows the fluorescence response toward decomplexation of **1** to “in situ”-generated **HL**.

$\times 10^3 \text{ M}^{-1} \text{ cm}^{-1}$), which has been attributed to the presence of **HL**, arising because of decomplexation of **1**. The presence of two isosbestic points at ~ 362 and $\sim 320 \text{ nm}$ also suggested the existence of a new chemical entity (**HL**) in the solution besides **1** and Cu^{2+} (Figure 6b). At this stage, the band due to the $n-\pi^*$ transition almost disappeared, leaving a residual hump, while the one at 281 nm ($\pi-\pi^*$) blue-shifted to appear at 274 nm ($\Delta\lambda, 07 \text{ nm}$). Furthermore, in the presence of 1.0 equiv of Hg^{2+} , the spectrum showed good resemblance with **HL**;

however, a residual hump indicated either incomplete decomplexation of Cu^{2+} from **1** or a competitive approach of Cu^{2+} with Hg^{2+} toward complexation (Figure 7d). Further additions of Hg^{2+} (1.0–3.0 equiv) exhibited changes similar to that arising from the interaction of Hg^{2+} with **HL** (Figure 6a,b). It clearly suggested that, after decomplexation, **HL** is generated in situ and further undergoes Hg^{2+} -induced hydrolysis at the aldimine core. Ultimately, at saturation, the spectra resembled well the one obtained from the treatment of Hg^{2+} with **HL** or

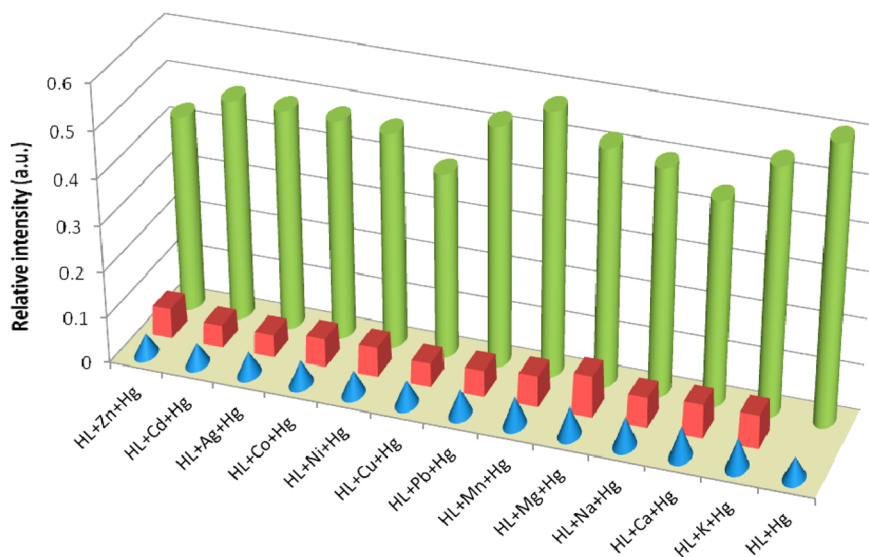


Figure 9. Fluorescence response of **HL** [c , 10 μM ; 9:1 (v/v) MeOH/H₂O] toward various metal ions (100 mM). Blue cones represent the emission intensities of free **HL**, brown bars intensity change in the presence of tested metal ions (10.0 equiv), and green cylindrical bars the subsequent addition of Hg²⁺ (1.0 equiv) to the same solution. The intensities were recorded at $\lambda_{\text{em}} = 423$ nm at rt.

DEA itself (Figures 6b and 4b). It is noteworthy to mention that the resulting species was isolated and characterized as DEA using ¹H NMR and mass spectrometry (SI, Figures S15b and S16). Also, interference studies demonstrated insignificant changes in the spectral features of **1** + Hg²⁺ in the presence of competing metal ions, which establishes **1** as a selective chemodosimeter for Hg²⁺ (Figure 7c).

To gain deep insight into the proficiency of **HL** and **1** toward a “turn-on” response for Hg²⁺, fluorescence titration experiments have been performed under analogous conditions (Figure 8). The addition of Hg²⁺ (0.2 equiv) to a solution of **HL** induced a ~3-fold increase in the fluorescence intensity. The limit of quantification of **HL** for Hg²⁺ was ~1.0:0.2 to ~1.0:2.0, and maximum fluorescence enhancement (~20-fold) was observed at ~1.0:2.0 (**HL**/Hg²⁺), wherein Φ was considerably enhanced to 0.43 (Figure 8a). Observed emission enhancement has been attributed to the formation of DEA via selective hydrolysis of the aldimine linkage despite the presence of ester groups in **HL** (SI, Figure S7). Job’s plot analysis revealed 1:1 stoichiometry between **HL** and Hg²⁺ (SI, Figure S8).

Likewise, the addition of Hg²⁺ (0.0–1.0 equiv) to a solution of **1** exhibited gradual fluorescence enhancement (~3-fold) and a small increase in the QY (Φ , 0.016; $\Delta\Phi = 0.005$; Figure 8b, inset). The slower response of **1** toward Hg²⁺ may be ascribed to decomplexation of Cu²⁺ to generate **HL**. A further addition of Hg²⁺ (1.2 equiv) displayed a sharp fluorescence enhancement (~7-fold; Φ , 0.077), probably because of initiation of hydrolysis of “in situ”-generated **HL**. An increase in the concentration of Hg²⁺ (3.0 equiv) led to enormous fluorescence enhancement (Figure 8b). Notably, at the saturation stage (maximum hydrolysis), the intensity assumed ~80-fold enhancement and QY increased by a factor of ~55 (Φ , 0.62; SI, Figure S7b). Although it may be presumed that decomplexation and hydrolysis phenomena occur simultaneously in the solution, a sharp enhancement was observed only after the addition of more than 1.0 equiv of Hg²⁺. This indicated that the mentioned amount (1.0 equiv) of Hg²⁺ is required for competitive Cu²⁺ displacement from **1**. Further, the very rapid response toward Hg²⁺ may be associated with the

cumulative effect of the background presence of 1.0 equiv of Hg²⁺ and externally added Hg²⁺, which simultaneously interacts with **HL**. To ascertain this viewpoint, a time-dependent fluorescence experiment was performed on **HL** and **1** using an excess of Hg²⁺ (10.0 equiv). It was observed that a ~80% increase in the fluorescence intensity occurred in just ~2.0 min and virtual saturation after ~6.0 min (SI, Figure S9).

A competitive metal-ion selectivity study was performed by adding Hg²⁺ to a solution of **HL** and tested metal ions (10.0 equiv). A fluorescence response was noted at $\lambda_{\text{em}} = 423$ nm ($\lambda_{\text{ex}} = 338$ nm) and is presented as a bar diagram in Figure 9. This study revealed that the addition of individual metal ions causes an insignificant change in the fluorescence intensity of **HL**, which substantially increased upon the addition of Hg²⁺ (1.0 equiv). Conversely, the addition of tested metal ions (10.0 equiv) to solutions of **HL** + Hg²⁺ and **1** + Hg²⁺ exhibited insignificant changes (SI, Figure S10). These experiments not only suggested a minor background effect of the other metal ions but also indicated appreciably good selectivity of **HL** and **1** for Hg²⁺. They also eventually proved that only a small amount of Hg²⁺ (1.0 equiv) is sufficient over a large quantity of other metal ions (10.0 equiv). Further, it has been concluded that the emission intensity is proportional to the concentration of the hydrolyzed product, in turn, generated (DEA) and may be attributed to the lowering of PET. Thus, the overall results from the fluorescence titration studies are consistent with the conclusions drawn from UV/vis studies.³²

The association constants for **HL** and **1** in the presence of Hg²⁺ have been deduced following the Benesi–Hildebrand method. It came out to be $K_a^{\text{HL}} = 7.1 \times 10^4 \text{ mol}^{-1}$ and $K_a^{\text{1}} = 1.8 \times 10^6 \text{ mol}^{-1}$ (SI, Figure S11). The higher association constant for **1** may be associated with the greater affinity of **1** toward Hg²⁺ relative to **HL**. To examine the sensitivity of **HL** toward Hg²⁺, the limit of detection (LOD) has been evaluated by adding a fixed volume (50 μL) of Hg²⁺ (10^{-12} – 10^{-9} M) to a solution of **HL** (c , 10 μM). The LOD was estimated to be 8×10^{-10} M for Hg²⁺, below the acceptable level in drinking water (SI, Figure S12).^{5a}

One can presume anonymously that the selectivity of **HL** and sensitivity of **1** toward Hg²⁺ may be affected by harsh

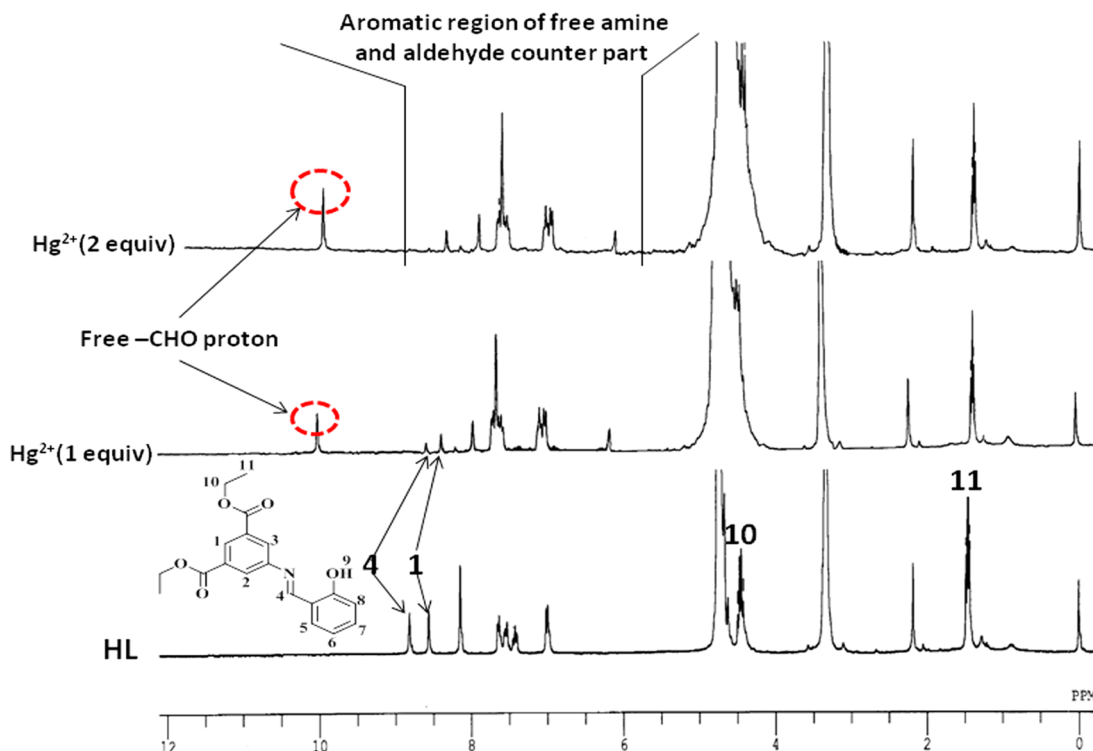


Figure 10. ^1H NMR titration spectra of **HL** with Hg^{2+} . The $-\text{OH}$ proton may not be visible because of fast exchange with a deuterated solvent.

competition between Hg^{2+} and Cu^{2+} . The spectral studies substantiated that the addition of only Hg^{2+} (hydrolysis) and Cu^{2+} (complex formation) to a solution of **HL** leads to significant spectral changes; these do not vie for each other because they are involved in two different phenomena. Ideally, the selectivity of **HL** for Hg^{2+} (hydrolysis) should not be significantly affected by the addition of Cu^{2+} (complex formation). On the other hand, the lower sensitivity of **1** for Hg^{2+} relative to **HL** has been ascribed to the use of the first mole ratio of Hg^{2+} for the decomplexation process, which, in turn, facilitates hydrolysis. Hg^{2+} does not tend to directly replace the coordinated Cu^{II} for complex formation, but rather it interacts only through the aldimine nitrogen ($-\text{N}=\text{CH}-$) to engage its lone pair of electrons for hydrolysis. It enhances polarity of the aldimine moiety, making the $-\text{N}=\text{CH}-$ carbon electropositive, and favors nucleophilic attack by H_2O . This reasonably explains negligible prospects for $[\text{Hg}(\text{L}_2)]$ formation, which has also been supported by the absence of the molecular ion peak associated with $[\text{Hg}(\text{L}_2)]$, or any species parallel to it in mass spectra of **1** + Hg^{2+} .

To gain deep insight into the selectivity/sensitivity of **HL/1**, a model compound (L_M) involving benzaldehyde instead of salicylaldehyde has been designed and synthesized (see the SI for details, Scheme S1 and Figure S3). Strategically, to eliminate the possibility of complex formation, the nitrogen/oxygen-donor chelating site was removed; however, to promote hydrolysis the aldimine bond was kept intact. As expected, the UV/vis and fluorescence spectra of L_M were significantly influenced only by Hg^{2+} and not Cu^{2+} /tested metal ions. The resultant spectral feature resembled to that of **DEA**, which notably indicates the selectivity of L_M for Hg^{2+} similar to **1** and not **HL** (an isolated absorption band like **HL** + Cu^{2+} did not appear). Conversely, the aliquot addition of Hg^{2+} led to significant changes in the UV/vis and fluorescence spectra of L_M , with the very first addition of Hg^{2+} (0.3 equiv) akin to **HL**

and saturated at 3.0 equiv (SI, Figure S13). This strongly suggested the significant role of Hg^{2+} in decomplexation of **1** and the comparable hydrolytic response of the aldimine core in L_M to that of **HL**. Notably, L_M required higher equivalents of Hg^{2+} (3.0 equiv) than **HL** (2.0 equiv of Hg^{2+}), which may be attributed to the absence of the *o*-OH substituent. In **HL**, the $-\text{OH}$ group offers greater electron density to ortho $-\text{N}=\text{CH}-$ nitrogen and facilitates interaction with Hg^{2+} , in turn, enhancing the sensitivity toward hydrolysis.

Effect of the pH. The pH sensitivity of aldimine linkages toward hydrolysis is well documented.³³ However, for a particular aldimine system, a short pH range may be effective and its stability may also depend on other factors including the effect of the substituents.³⁴ The compounds under investigation, **HL** and **1**, contain ester groups that stabilize that isophthalate ring with respect to the aldimine core. Conversely, ester groups also provide a potential site for hydrolysis under the influence of Hg^{2+} . During the UV/vis and fluorescence studies in the presence of Hg^{2+} (10.0 equiv), the pH of the systems varied from ~ 7.2 to ~ 5.2 for **HL** and from ~ 7.4 to ~ 4.9 for **1**. To investigate the effect of the pH in the absence of Hg^{2+} , pH titrations have been performed using 0.1 M HCl. The aliquot addition of HCl led to a gradual decrease in the pH of **HL** and **1** to ~ 2.5 and displayed no significant change in their absorption/emission spectra up to pH ~ 3.5 (SI, Figure S14). The above observations clearly indicated that hydrolysis of **HL** and **1** may be subjected to two different sites, aldimine ($-\text{CH}=\text{N}-$) and ester ($-\text{COOC}_2\text{H}_5$), yet Hg^{2+} plays a crucial role in triggering preferable hydrolysis of the $-\text{CH}=\text{N}-$ linkage over an ester group in a wide pH range. The solitary effect of an acidic pH imposed insignificant changes in the absorption/emission spectra of **HL** and **1**.³⁵ However, some irrelevant changes were observed in their fluorescence spectra below pH ~ 3.5 . These changes are entirely different from that

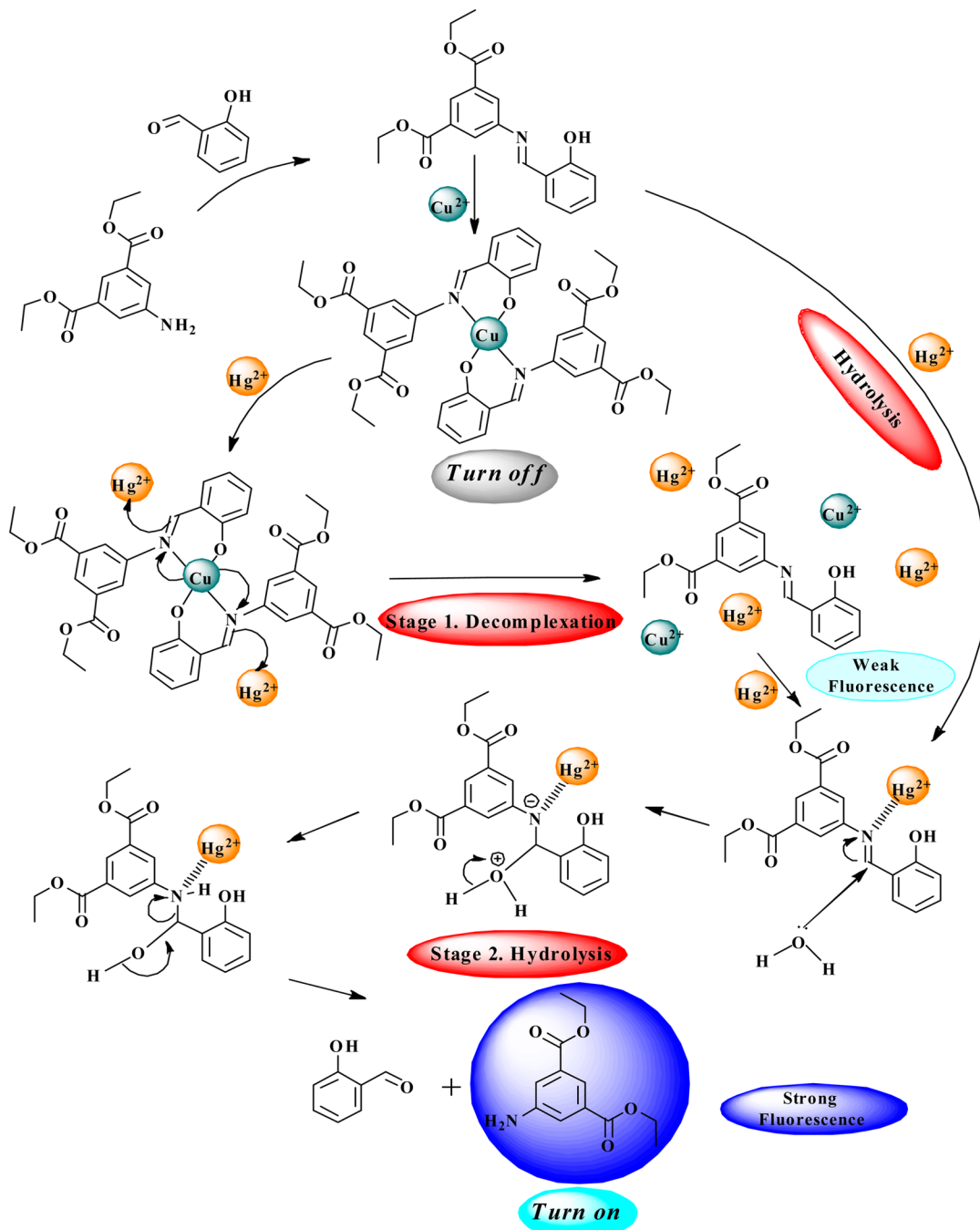


Figure 11. Plausible mechanism for Hg^{2+} detection via chemodosimetric transformations: complex formation (turn off); subsequent Hg^{2+} addition in two stages; stage 1, Hg^{2+} -induced Cu^{2+} displacement, leading to decomplexation, i.e., in situ generation of HL (weak fluorescence); stage 2, Hg^{2+} -assisted hydrolysis, leading to the formation of DEA (turn on).

observed with Hg^{2+} , which, in turn, supported the key role played by Hg^{2+} in hydrolytic transformations.³⁶

^1H NMR Studies. To have an idea about the mechanism of fluorescence enhancement in the presence of Hg^{2+} , ^1H NMR titrations have been performed using HL (CD_3OD) and an aqueous solution of Hg^{2+} (0.01 mM) as an analyte. Upon the addition of Hg^{2+} (1.0 equiv) to a solution of HL , resonances due to the aldimine proton $-\text{CH}=\text{N}-$ ($\text{H}4$, δ 8.82) significantly diminished and a new signal assignable to free aldehyde appeared at δ 9.97. Further additions of Hg^{2+} (~2.0 equiv) led to prominence of the resonances due to free aldehyde, while signals due to the azomethine proton

completely disappeared (Figure 10). This clearly indicated Hg^{2+} -induced hydrolysis of the aldimine bond. Moreover, it is worth mentioning that the addition of Hg^{2+} (1.0 equiv) leads to an almost negligible change for the signals due to the $-\text{CH}_2-$ ($\text{H}10$) and $-\text{CH}_3$ ($\text{H}11$) moieties of the ester resonating at δ 4.45 (q, 4H) and δ 1.46 (t, 6H). With an increase in the concentration of Hg^{2+} , the signals due to the $-\text{CH}_2-$ protons apparently merged with the solvent and retained its identity. In addition, aromatic protons corresponded to the characteristic resonances due to DEA and salicylaldehyde. The peak assignable to the $-\text{NH}_2$ proton was not observable, probably because of its merger with the solvent peak. A ^1H NMR

titration study clearly suggested that the addition of Hg^{2+} could impose significant changes, particularly for protons due to the aldimine linkage, and the hydrolyzable ester group remained intact. On the other hand, a well-resolved ^1H NMR spectrum for **1** could not be obtained because of a paramagnetic $\text{Cu}^{2+}(\text{d}^9)$ system.³⁷

Mass Spectral Studies. ESI-MS of **HL** displayed a molecular ion peak at m/z 342.1518 [$(\text{M} + \text{H})^+$; 100%] along with other peaks at m/z 382.1441 [$(\text{M} + \text{Na} + \text{H}_2\text{O})^+$; 40%], 364.1343 [$(\text{M} + \text{Na})^+$; 28%], and 705.2711 [$(2\text{M} + \text{Na})^+$; 4%] (SI, Figure S4a). Similarly, **1** in its ESI-MS displayed a molecular ion peak at m/z 745.2052 [$(\text{M} + \text{H})^+$; 15%] and prominent peaks at m/z 342.1473 [$(\text{L} + 2\text{H})^+$; 100%] and 705.2671 [$\{\text{2(L} + \text{H}) + \text{Na}\}^+$; 45%] (SI, Figure S4b). The presence of various peaks and their position strongly supported the formulation of **HL** and **1**. To have an idea about the composition of the species resulting from the interaction of **HL** + Hg^{2+} and **1** + Hg^{2+} , ESI-MS of the isolated products were acquired. Notably, products from both the former and latter exhibited a 100% intense peak at m/z 238.1012 and 238.1107, respectively (SI, Figure S15a,b). This signifies that **HL** and **1** upon treatment with Hg^{2+} ended up with the same species, i.e., DEA (calcd m/z 238.1035), and strongly suggested that Hg^{2+} -induced hydrolysis of the aldimine linkage occurred in **HL** as well as in **1**. Therefore, one may conclude that these exhibit 100% feasibility of being hydrolyzed by Hg^{2+} in mixed-aqueous media.

On the basis of the above observations, a plausible mechanism for Hg^{2+} -assisted hydrolysis of **HL** and **1** has been proposed (Figure 11). In the presence of Hg^{2+} , **HL** directly undergoes hydrolysis at the aldimine linkage, while **1** in the very first step undergoes decomplexation (stage 1) and the resulting species passes through hydrolytic cleavage (stage 2) at the aldimine linkage. Stage 2 is mechanistically similar to direct hydrolysis of **HL**, and that is why **HL** and **1** exhibit analogous spectral features under the influence of Hg^{2+} and end up with the same product, DEA, which is liable for a highly fluorescent “switch-on” response.

CONCLUSIONS

In summary, through this work, the synthesis and spectral and structural characterization of a new Schiff base, **HL**, and a copper(II) complex, **1**, derived from it have been described. These exhibit appreciable chemodosimetric behavior toward Hg^{2+} via hydrolytic cleavage of the aldimine linkage. The actual moiety involved in chemodosimetric detection has been identified as **HL**, and the concept of hydrolysis is well supported by synthesizing complex **1** bearing **HL**, which markedly displays similar chemodosimetric behavior via magnificent decomplexation by Hg^{2+} . Various competitive experiments have been carried out, and the results strongly support the proposed theme. Chemodosimeters presented through this work are quite sensitive and show tremendous selectivity toward Hg^{2+} through site-specific hydrolysis. In other words, these provide an opportunity for Hg^{2+} to opt a site for hydrolysis between ester and aldimine linkage under analogous conditions. The present work may be used as a prototype in the field of Hg^{2+} -assisted chemodosimeter hydrolysis in aldimine systems and can be further extended to develop a new class of chemodosimeters.

ASSOCIATED CONTENT

Supporting Information

Characterization data, UV-vis and fluorescence spectra related to this work, and crystal data file in CIF format (CCDC 955431 and 955432 for **HL** and complex **1**, respectively). This material is available free of charge via the Internet at <http://pubs.acs.org>.

AUTHOR INFORMATION

Corresponding Author

*E-mail: dspbhu@bhu.ac.in. Tel.: + 91 542 6702480. Fax: + 91 542 2368174.

Notes

The authors declare no competing financial interest.

ACKNOWLEDGMENTS

The authors thank the Council of Scientific and Industrial Research, New Delhi, India, for financial assistance through Scheme HRDG 01 (2361/10/EMR-II) and the Department of Science and Technology, New Delhi, India, through Scheme IFA12-CH-66. A.K. thanks the University Grants Commission, New Delhi, India, for a Senior Research Fellowship [R/Dev./Sch.(UGC-JRF-SRF)/S-01:29.2.29]. We are also thankful to the Head, Department of Chemistry, Faculty of Science, Banaras Hindu University, Varanasi (U.P.), India, for extending laboratory facilities. The authors also thank Prof. R. Murugavel for extending his X-ray Single Crystal Diffraction Facility, established through a DAE-SRC Outstanding Investigator Award.

REFERENCES

- Loon, G. W.; Duffy, S. J. *A Global Perspective. Environmental Chemistry*; Oxford University Press: Oxford, U.K., 2000.
- Schrope, M. *Nature* **2001**, *409*, 124–124.
- Yoshizawa, K.; Rimm, E. B.; Morris, J. S.; Spate, V. L.; Hsieh, C. C.; Spiegelman, D.; Stampfer, M. J.; Willett, W. C. *New Engl. J. Med.* **2002**, *347*, 1755–1760.
- (a) Wang, Q. R.; Kim, D.; Dionysiou, D. D.; Sorial, G. A.; Timberlake, D. *Environ. Pollut.* **2004**, *131*, 323–336. (b) Dias, G. M.; Edwards, G. C. *Hum. Ecol. Risk Assess.* **2003**, *9*, 699–721.
- (a) U.S. EPA Regulatory Impact Analysis of the Clean Air Mercury Rule: EPA-452/R-05-003, Research Triangle Park, NC, 2005. (b) Clarkson, T. W.; Magos, L.; Myers, G. J. *New Engl. J. Med.* **2003**, *349*, 1731–1737. (c) Mottet, N. K.; Vahter, M. E.; Charleston, J. S.; Friberg, L. T. *Met. Ions Biol. Syst.* **1997**, *34*, 371–403. (d) Davidson, P. W.; Myers, G. J.; Cox, C.; Axtell, C.; Shamlaye, C.; Sloane-Reeves, J.; Cernichiari, E.; Needham, L.; Choi, A.; Wang, Y.; Berlin, M.; Clarkson, T. W. *J. Am. Med. Assoc.* **1998**, *280*, 701–707. (e) Harada, M. *Crit. Rev. Toxicol.* **1995**, *25*, 1–24.
- (a) Edward, A. N.; David, F. G. *Nature* **1992**, *358*, 139–141. (b) Nolan, E. M.; Lippard, S. J. *Chem. Rev.* **2008**, *108*, 3443–3480.
- (7) (a) Boening, D. W. *Chemosphere* **2000**, *40*, 1335–1351. (b) Benoit, J. M.; Fitzgerald, W. F.; Damman, A. W. *Environ. Res.* **1998**, *78*, 118. (c) Queen, H. L. *Chronic Mercury Toxicity: New Hope Against An Endemic Disease*; Queen and Company Health Communications, Inc.: Colorado Springs, CO, 1998. (d) Renzoni, A.; Zino, F.; Franchi, E. *Environ. Res.* **1998**, *77*, 68.
- (8) (a) Grandjean, P.; Weihe, P.; White, R. F.; Debes, F. *Environ. Res.* **1998**, *77*, 165. (b) Takeuchi, T.; Morikawa, N.; Matsumoto, H.; Shiraishi, Y. *Acta Neuropathol.* **1962**, *2*, 40. (c) Harada, M. *Crit. Rev. Toxicol.* **1995**, *25*, 1.
- (9) (a) Bag, B.; Bharadwaj, P. K. *Inorg. Chem.* **2004**, *43*, 4626–2630. (b) Varnes, A. W.; Dodson, R. B.; Wherry, E. L. *J. Am. Chem. Soc.* **1972**, *94*, 946–950. (c) McClure, D. S. *J. Chem. Phys.* **1952**, *20*, 682–686.
- (10) (a) Pandey, R.; Gupta, R. K.; Shahid, M.; Maiti, B.; Misra, A.; Pandey, D. S. *Inorg. Chem.* **2012**, *51*, 298–311. (b) Gupta, R. K.;

- Pandey, R.; Singh, R.; Srivastava, N.; Maiti, B.; Saha, S.; Li, P.; Xu, Q.; Pandey, D. S. *Inorg. Chem.* **2012**, *51*, 8916–8930.
- (11) Guo, X. F.; Jia, L. H.; Qian, X. H. *J. Am. Chem. Soc.* **2004**, *126*, 2272–2273.
- (12) Chen, X. Q.; Nam, S. W.; Jou, M. J.; Kim, Y.; Kim, S. J.; Yoon, J.; Park, S. *Org. Lett.* **2008**, *10*, 5235–5238.
- (13) He, G. J.; Zhao, Y. G.; He, C.; Liu, Y.; Duan, C. Y. *Inorg. Chem.* **2008**, *47*, 5169–5176.
- (14) Wu, D. Y.; Huang, W.; Lin, Z. H.; Duan, C. Y.; He, C.; Wu, S.; Wang, D. H. *Inorg. Chem.* **2008**, *47*, 7190–7201.
- (15) Al-Kady, A. S.; Gaber, M.; Hussein, M. M.; Ebeid, E. Z. M. J. *Phys. Chem. A* **2009**, *113*, 9474–9484.
- (16) Long, Y. F.; Jiang, D. L.; Zhu, X.; Wang, J. X.; Zhou, F. M. *Anal. Chem.* **2009**, *81*, 2652–2657.
- (17) (a) Warther, D.; Bolze, F.; Leonard, J.; Gug, S.; Specht, A.; Puliti, D.; Sun, X. H.; Kessler, P.; Lutz, Y.; Vonesch, J. L.; Winsor, B.; Nicoud, J. F.; Goeldner, M. *J. Am. Chem. Soc.* **2010**, *132*, 2585–2590. (b) Kumar, N.; Bhalla, V.; Singh, H.; Sharma, P. R.; Kaur, T.; Kumar, M. *Org. Lett.* **2011**, *13*, 1422–1425.
- (18) (a) Wegner, S. V.; Okesli, A.; Chen, P.; He, C. A. *J. Am. Chem. Soc.* **2007**, *129*, 3474–3475. (b) Guo, C. L.; Irudayaraj, J. *Anal. Chem.* **2011**, *83*, 2883–2889. (c) Wen, D.; Deng, L.; Guo, S. J.; Dong, S. J. *Anal. Chem.* **2011**, *83*, 3968–3972.
- (19) (a) Kim, Y. J.; Johnson, R. C.; Hupp, J. T. *Nano Lett.* **2001**, *1*, 165–167. (b) Jin, Y. D.; Shen, Y.; Dong, S. J. *J. Phys. Chem. B* **2004**, *108*, 8142–8147. (c) Sun, H. Z.; Wei, H. T.; Zhang, H.; Ning, Y.; Tang, Y.; Zhai, F.; Yang, B. *Langmuir* **2011**, *27*, 1136–1142.
- (20) (a) Chea, M. Y.; Czarnik, A. W. *J. Am. Chem. Soc.* **1992**, *114*, 9704–9705. (b) Du, J. J.; Fan, J. L.; Sun, P. P.; Wang, J. Y.; Li, H. L.; Sun, S. G.; Peng, X. J. *Org. Lett.* **2010**, *12*, 476–479.
- (21) Bhalla, V.; Mehto, R.; Kumar, M.; Sharma, P. R.; Kaur, T. *Dalton Trans.* **2013**, *42*, 15063–15068.
- (22) Perrin, D. D.; Armango, W. L. F.; Perrin, D. R. *Purification of Laboratory Chemicals*; Pergamon: Oxford, U.K., 1986.
- (23) Bergbreiter, D. E.; Frels, J. D.; Rawson, J.; Li, J.; Reibenspies, J. H. *Inorg. Chim. Acta* **2006**, *359*, 1912–1922.
- (24) Sheldrick, G. M. *SHELXL-97, Program for X-ray Crystal Structure Refinement*; Göttingen University: Göttingen, Germany, 1997.
- (25) Maus, M.; Rettig, W.; Bonafoix, D.; Lapouyade, R. *J. Phys. Chem. A* **1999**, *103*, 3388–3401.
- (26) Desiraju, G. R.; Steiner, T. *The Weak Hydrogen Bond in Structural Chemistry and Biology*; Oxford University Press: Oxford, U.K., 1999.
- (27) Pauling, L. *The Nature of the Chemical Bond*, 3rd ed.; Cornell University Press: New York, 1960. Curry, J. D.; Jandacer, R. J. *J. Chem. Soc., Dalton Trans.* **1972**, 1120.
- (28) (a) Karabiyik, H.; Erdem, O.; Aygun, M. *J. Inorg. Organomet. Polym.* **2010**, *20*, 142. (b) Mukherjee, P.; Drew, M. G. B.; Figuerola, A. *Polyhedron* **2008**, *27*, 3343. (c) Mouni, L.; Akkurt, M.; Yildirm, S. O. *J. Chem. Crystallogr.* **2010**, *40*, 169.
- (29) Reddy, P. R.; Shilpa, A. *Chem. Biodiversity* **2012**, *9*, 2262.
- (30) (a) Quang, D. T.; Kim, J. S. *Chem. Rev.* **2010**, *110*, 6281. (b) Ros-Lis, J. V.; Marcos, M. D.; Mez, R. M.; Rurack, K.; Soto, J. *Angew. Chem., Int. Ed.* **2005**, *44*, 4405–4407.
- (31) Zhang, B. G.; Xu, J.; Zhao, Y. G.; Duan, C. Y.; Cao, X.; Meng, Q. *J. Dalton Trans.* **2006**, 1271–1276.
- (32) Xu, Z.; Han, S. J.; Lee, C.; Yoon, J.; Spring, D. R. *Chem. Commun.* **2010**, *46*, 1679–1681.
- (33) Wang, Z.; Möhwald, H.; Gao, C. *ACS Nano* **2011**, *5*, 3930–3936.
- (34) El-Taher, M. A. E. *J. Solution Chem.* **1996**, *25*, 401–410.
- (35) Lee, M. H.; Cho, B.; Yoon, J.; Kim, J. S. *Org. Lett.* **2007**, *9*, 4515–4518.
- (36) Tatay, S.; Gavin, P.; Coronado, E.; Palomares, E. *Org. Lett.* **2006**, *8*, 3857–3860.
- (37) (a) Hernández-Molina, R.; Mederos, A.; Gili, P.; Domínguez, S.; Lloret, F. *J. Chem. Soc., Dalton Trans.* **1997**, 4327–4334. (b) Pardo, E.; Ruiz-García, R.; Lloret, F.; Julve, M.; Cano, J.; Pasà, J.; Ruiz-Pérez, C.; Filali, Y.; Chamoreau, L.-M.; Journaux, Y. *Inorg. Chem.* **2007**, *46*, 4504–4514. (c) Palacios, M. A.; Rodríguez-Dieguez, A.; Sironi, A.; Herrera, J. M.; Mota, A. J.; Cano, J.; Colacio, E. *Dalton Trans.* **2009**, 8538–8547.